Journal of Atmospheric and Solar-Terrestrial Physics 140 (2016) 16–22

Contents lists available at ScienceDirect

Journal of Atmospheric and Solar-Terrestrial Physics

journal homepage: www.elsevier.com/locate/jastp

Research paper

Atmospheric changes observed during April 2015 Nepal earthquake

Nandita D. Ganguly

St. Xavier's College, Navrangpura, Ahmedabad 380009, Gujarat, India

ARTICLE INFO

Article history:
Received 2 November 2015
Received in revised form
29 January 2016
Accepted 30 January 2016
Available online 1 February 2016

Keywords:
Pressure
Aerosol index
Aerosol optical depth
NO_2
Ozone

ABSTRACT

A massive earthquake shook Nepal on 25 April 2015, with a moment magnitude of 7.9 M_w, its hypocenter at a depth of 10 km. Atmospheric changes that precede an earthquake might offer the hope of early warning and evacuation. Although the existence of such precursory signals is highly controversial, an attempt has been made to investigate the atmospheric changes from two months prior, to five months following this deadly earthquake. Aerosol optical depth (AOD) and columnar ozone were found to be higher by 40% and 6% respectively prior to the occurrence of the earthquake. The UV aerosol index (UVI), AOD and columnar NO_2 increased, while columnar ozone and sea level pressure dropped following the earthquake.

1. Introduction

A massive earthquake (Gorkha earthquake) lasting around twenty second shook Nepal at 11:56 NST on 25 April 2015, with a moment magnitude of 7.9 M_w and a Mercalli Intensity of VIII (Severe). Its epicenter (28.1°N, 84.6°E), was the village of Barpak, Gorkha district situated upon the hilltop (about 1900 m above sea level), and its hypocenter at a depth of approximately 10 km. Being a shallow earthquake; it caused severe damage to life and property and was perhaps the worst natural disaster to strike Nepal since the earlier 1934 quake. The earthquake triggered an avalanche on Mount Everest and in the Langtang valley, killed and rendered thousands of people homeless, flattened entire villages, destroyed centuries-old buildings, lifted areas near the city of Kathmandu by around 3 feet and reduced the height of Mount Everest by about an inch. Tremors were also felt in northern parts of India. Around 200 aftershocks followed thereafter for several months, among which the strongest occurred on 12 May 2015 at 12:51 NST with a magnitude of 7.3 M_w (Fig. 1). Although the frequency of aftershocks decreased gradually with time, the depth of focus for most aftershocks remained around 10 km from the earth's surface and its magnitude also remained around 4 M_w up to Sep 7 2015. According to the United States Geological Survey (USGS; http://www.usgs.gov/), the principal earthquake was caused by a sudden thrust, or release of built-up stress, along the major fault line where the Indian plate is slowly diving underneath the Eurasian plate. Kathmandu, situated on a block of crust approximately 120 km wide and 60 km long, reportedly shifted 3 m to the south in just 30 s. The earthquake's effects were amplified in Kathmandu, which lies on the Kathmandu Basin, containing up to 600 m of sedimentary rocks.

Changes in columnar water vapor (Dey et al., 2004), columnar ozone (Ganguly, 2009), aerosol parameters (Okada et al., 2004; Qin et al., 2014a), surface changes, change in water color (Singh et al., 2002) and evaporation rate (Singh and Ouzounov, 2003; Dey and Singh, 2003), has been widely reported prior to and during earthquakes. Singh et al., (2010) have reported that changes in the subsurface stress result in changes in the hydrological regime, which in turn causes emission of greenhouse gases like, Carbon monoxide (CO), Carbon dioxide (CO_2), Oxides of Nitrogen ($NO_x = N + NO + NO_2$) and Methane (CH_4) from the epicentral region. High electric fields have been found over seismically active regions a few days prior to strong earthquakes, which is believed to penetrate into the ionosphere and create specific irregularities of electron concentrations over the active regions (Singh et al., 2007), and it also leads to a large amount of particle precipitation at stratospheric altitudes (Tertyshinikov, 1996). Surface latent heat flux enhancements around 11 days prior to the Pu'er earthquake in China had been reported by Qin et al., (2014b), which had good spatial correspondence with the epicenter and the local active faults. In the light of these observations, this paper is aimed to investigate the atmospheric changes associated with the deadly 2015 Nepal earthquake.

2. Data and measurements

Daily 1°Lat × 1°Lon gridded aerosol optical depth for 550 nm (Region 83°E–86°E, 27°N–29°N) has been retrieved from the Moderate Resolution Imaging Spectroradiometer (MODIS) Terra research satellite. MODIS tracks a wider array of the earth's vital signs than any other TERRA sensor. Tropospheric column amount

http://dx.doi.org/10.1016/j.jastp.2016.01.017
1364-6826/

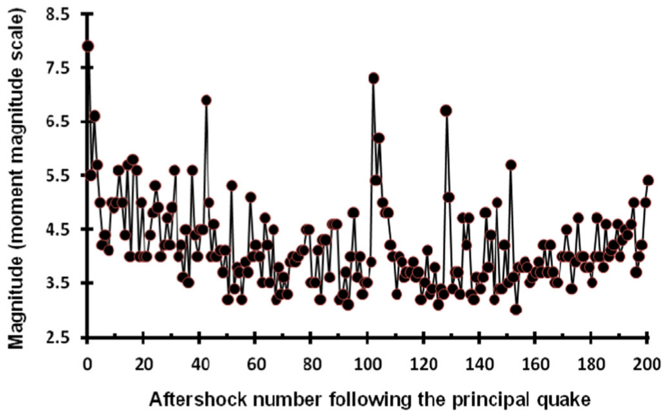

Fig. 1. Plot of aftershock number following the principal quake versus their corresponding magnitude on moment magnitude scale. The principal quake, which occurred on 25 April 2015, is denoted by the number zero.
(*Source of data:* India Meteorological Department).

NO_2, UV aerosol index and Column amount ozone (Region 83°E–86°E, 27°N–29°N) have been retrieved from the Aura mission Ozone Monitoring Instrument (OMI) version 3 daily global data products. The OMI data are binned to 0.25°Lat × 0.25° Lon grids. These datasets have been filtered by good quality and all data pixels, which fall within a grid cell, are stored without averaging (Ahmad et al., 2004; Vasilkov et al., 2008). Analyses and visualizations used in this paper were produced with the Giovanni online data system (Acker and Leptoukh, 2007). The sea level pressure data from automated weather station operating at Tribhuvan International airport, Kathmandu (27.7°N, 85.33°E; 184 km from epicenter) has been obtained from the website www.wunderground.com. This data is updated hourly. Whenever data for Tribhuvan airport was not available during the earthquake, the data for geographically closest Personal Weather Station (PWS) maintained at Patan, Lalitpur, Nepal located 5 km away from Kathmandu was considered. According to weather wunderground, these PWS data are put through strict quality control and observations are updated as often as every 2.5 s. The general features of the earthquake and its aftershocks such as magnitude, depth of focus, and day of occurrence have been obtained from the website of India Meteorological Department (http://www.imd.gov.in/pages/earthquake_prelim.php).

3. Results and discussions

The UV aerosol index (UVI), aerosol optical depth (AOD), columnar NO_2, columnar O_3 and sea level pressure (P) observed on each individual day has been subtracted from that observed on the day of the earthquake to obtain the changes ΔUVI, ΔAOD, ΔNO_2, ΔO_3 and ΔP respectively. The time series of these changes have been plotted over the period from two months prior to the occurrence of earthquake to five months following the earthquake.

3.1. Change in sea level pressure

Time series of ΔP measured at Tribhuvan International airport, Kathmandu (27.7°N, 85.33°E; 184 km from epicenter) is plotted in Fig. 2. It is observed that ΔP dropped sharply, following the earthquake and during the period of aftershocks. This may be due to the pressure change driven by vertically upward propagating infrasonic waves, generated by the seismic Raleigh waves passing by the site, as suggested by Watada et al. (2006).

3.2. Change in UV aerosol index and Aerosol optical depth

UVI detects the presence of uv-absorbing aerosols such as dust and soot. AOD is a measure of the extinction of the solar beam by dust and haze (smoke, pollution).

Abnormal ionospheric disturbances associated with earthquakes have been reported extensively (Liu et al., 2009; Blecki et al., 2010; Lin., 2011). One of the possible mechanisms of seismo-ionospheric effects is seismogenic electric field, which is connected with the vertical turbulent transfer of charged aerosols injected in atmosphere and air ionization by radon followed by formation of large ion clusters of aerosol size during the preparation of an earthquake (Qin et al., 2014a). Time series of ΔAOD (Fig. 3a) indicated an enhancement of 0.9 in AOD at 550 nm, 26 days prior to the occurrence of the earthquake which was localized to the region of earthquake (Fig. 3b). Similar enhancement of AOD along the Longmenshan faults was observed by Qin et al. (2014a), 7 days before the 2008 Wenchuan earthquake, which was also localized to the region of earthquake and correlated well with the active faults and surface ruptures. They have suggested that this unique enhancement could be associated with the Lithosphere-Atmosphere-Ionosphere coupling process during the preparatory stage of the earthquake.

ΔAOD and ΔUVI increased by factors of 0.6 and 2.3 respectively (Figs. 3a and 4a) following the earthquake. This may be attributed to the emission of dust into the atmosphere following the collapse of buildings and large scale destruction triggered by the earthquake and its aftershocks. Image of the spatial distribution of UVI (Fig. 4b) shows enhanced UVI around the epicenter following the earthquake. The Indo-Gangetic plains bordering Nepal shown in Figs. 3b and 4b exhibit higher AOD and UVI than the epicenter because; even under normal conditions, these regions have high

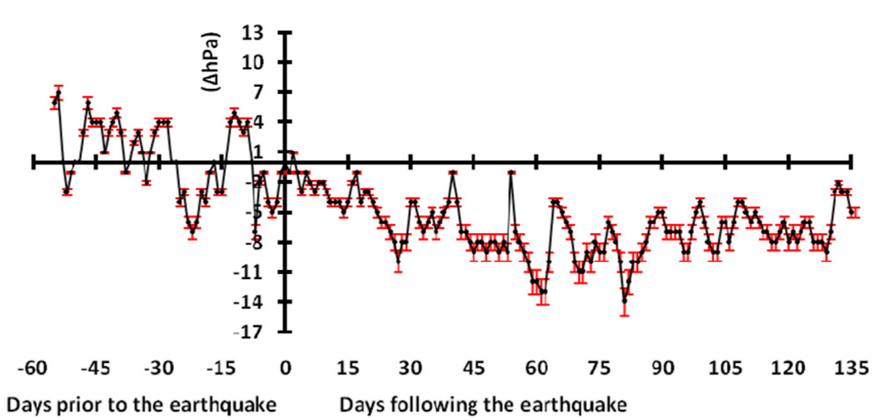

Fig. 2. Time series of the change in sea level pressure (ΔP) with respect to the sea level pressure on the earthquake day at Tribhuvan International airport, Kathmandu (*Source of data:* weather wunderground). Bars indicate 10% error.